Supporting Information

Li et al. 10.1073/pnas.0901754106

SI Materials and Methods

Cell Culture and Transfection. *Leishmania major* LC-8 gene was PCR-amplified from *L. major* genomic DNA with the primers 5′-TCC**GGATCC**CCACTGCTCCGCCATCTTG-3′ and 5′-TCC**GGATCC**ATGAAGCGGACATGTCG-3′ (restriction sites added are in boldface), and the product was digested with *Bam*HI and inserted into the pX-derived pMRP1-TAP vector. *Leishmania tarentolae* cells were transfected and selected for G418 resistance. The transfected cells were cultured in brain heart infusion medium with 10 μg/mL hemin and 100 μg/mL geneticin in a BioFlo 4500 Fermentor (New Brunswick Scientific). Late log phase cell cultures were harvested, and the cell pellets were kept at −80 °C.

TAP Isolation of L-complex. Tandem affinity purification was performed from whole cells. A cell pellet (≈50-g wet weight) was lysed in 200-mL TMK buffer (20 mM Tris pH 7.6, 60 mM KCl, 10 mM $MgCl_2$) containing 0.5% Triton X-100. The clarified cell lysate was incubated with 1.8-mL-washed IgG Sepharose for 3 h. The resin was transferred to a 10-mL column and washed with TKM buffer. The resin was then incubated with TEV protease for 14 h at 5 °C. The TEV released material was then bound to 400-μL calmodulin resin and released with EGTA. The eluted protein complex was concentrated to 500 μL in a Microcon YM-100 centrifugal filter (Millipore). The sample was then applied to a Superose 6 10/300 GL column (Amersham Biosciences) previously equilibrated with TMK buffer. Chromatography was performed on an AKTA Explorer 100 system (GE Healthcare) with 0.5 mL/min flow rate and fraction size of 0.5 mL.

In vitro editing assays were performed as described in refs. 1–3. The purified L-complex fractions were incubated with synthetic RNAs. The mRNAs were either 5′-end-labeled by using T4 polynucleotide kinase (Invitrogen) and [α-^{32}P]ATP or 3′-end-labeled by using T4 ligase and [α-^{32}P]pCp. Reactions were performed in 20 mM HEPES, pH 7.9, 10 mM $MgCl_2$, 10 mM KCl, 1 M DTT in the presence of RNase inhibitor at 27 °C for 120 min, and the products were analyzed on an 8 M urea, 15% polyacrylamide gel.

To obtain antibody-decorated particles, anti-REL1 monoclonal IgG was incubated with the TAP-purified particles for 30 min on ice before Superose 6 chromatography. The peak fractions were selected for tomographic analysis.

Western Blotting. Electrophoretic transfer on nitrocellulose membrane for SDS gels and on Immobilon P filter (Millipore) for blue native gels was performed for 1.5 h in Mini TransBlot cells (Bio-Rad Laboratories) in 25 mM Tris, 190 mM glycine, 10% methanol at 80 V. Immobilon filter was soaked in methanol and then in transfer buffer. Gels and membrane were presoaked in transfer buffer for 10 min before blotting. Immunodetection was performed with affinity-purified rabbit antibody and SuperSignal West Pico chemiluminescent substrate (Pierce) by standard techniques. Membrane blocking and antibody incubations were done in 5% milk in PBS buffer, pH 7.5, with 0.05% Tween 20 for 1 h, and all washes were in 1× PBS/0.05% Tween 20.

Mass Spectrometry Analysis. In-gel tryptic digestion and mass spectrometry: Protein bands excised from SDS-acrylamide gels were crushed, washed in 25 mM ammonium bicarbonate/50% acetonitrile, dried, reduced, derivatized with iodoacetamide, and digested with trypsin by standard methods. The recovered tryptic peptides were adsorbed onto μC^{18} ZipTips (Millipore), washed with 0.1% TFA, then eluted with 3–4-μL 50% ACN/0.1% TFA. One microliter tryptic peptide mixture from each gel band was combined with an equal volume of matrix solution and allowed to dry on the MALDI target. The matrix solution used was a 10 g/L solution of α-cyano-4-hydroxycinnamic acid in 50% acetonitrile/50% 0.1% aqueous TFA. All mass spectrometric measurements were performed on a 4700 Proteomics Analyzer (Applied Biosystems), which is a tandem time-of-flight instrument (TOF/TOF) with a MALDI ion source (4). Normal reflector spectra were acquired first to determine the masses of the peptides of interest. Trypsin autolysis peaks were used to calibrate the mass scale, typically giving masses to better than 10 ppm accuracy. MS/MS CID spectra were acquired manually on selected peptides, using air as the collision gas. Default calibration of the mass scale was used for all MS/MS spectra, which typically provided fragment masses accurate to <0.1 Da. Peptide sequences were determined by manual interpretation of the MS/MS spectra. Calculated masses of the sequences determined were checked against the experimental accurate masses to verify that they were consistent. In most instances (about 60%–70%), I and L could be distinguished by the presence of w ions. Q and K could usually be determined from the accurate mass of the whole peptide. The sequences determined were searched by using Protein Prospector [University of California, San Francisco (UCSF)] against the National Center for Biotechnology Information database as well as the parasite genome databases at http://www.genedb.org.

Electron Tomography (ET). A total of 17 ET tilt series was collected on a FEI Tecnai TF20 at an accelerating voltage of 200 kV using the FEI *Batch Tomography* program. The instrument is equipped with a 16-megapixel CCD camera. Tilt angles ranging from −70° to 70° were chosen according to the cosine scheme. The magnification used was 40,600× with 2 binning, giving a final sampling pixel size of 7.4 Å/pixel. The underfocus value of the zero-tilt image was set to 3 μm.

For data processing, we first used the *Inspect3D* tomography reconstruction package from FEI to perform a translational and rotational alignment, tilt axis refinement, and 3D reconstruction. We then refined the tomograms using the *ProTomo* package (5) iteratively until no significant improvement in the alignment parameters and the 3D volume was detectable. The final 3D map was then computed by the weighted back projection algorithm in the *ProTomo* package (5).

Transmission Electron Microscopy and Single-Particle Reconstruction. The purified L-complex sample was examined by negative stain transmission electron microscopy. A droplet of sample was placed on a carbon-coated copper grid, blotted from the grid edge, immediately stained with 2% uranyl acetate for 2 min, and washed 3 times with the staining solution. Each selected sample area was imaged 10 times with low dose (≈20 electrons/Å^2/exposure) in a FEI TF20 electron microscope operated at 200 kV on a TVIPS 16-megapixel CCD camera at 70,000× total magnification. The 10 images were aligned and averaged to enhance the signal-to-noise ratio. We found that we could improve the signal-to-noise ratio of the same image by averaging multiple low-dose shots of the same sample area. Adding >10 shots did not improve the signal further. The final step size was 2.143 Å/pixel.

Image classification and single-particle reconstruction were

performed with the EMAN package (6). Particle images were semiautomatically selected with the boxer program. Selected particle images were first subjected to a 2D classification to assess the size, shape, and homogeneity of the particles. They were then subjected to a projection-matching based refinement process with a Gaussian sphere as the initial model. A total of 8 iterations were used until the structure converged to a stable model and no further improvement was observed. The matching between projection and class averages of the last iteration were visually inspected for similarity (Fig. S2). The orientation distribution of the final classes is shown in Fig. S4. The effective resolution of the final reconstruction was estimated by using the 0.5 cut-off criterion of the Fourier shell correlation coefficient.

As an independent validation of the single-particle reconstruction, we also aligned the same data set by using the averaged tomographic structure filtered to 100 Å as an initial model. The same iterative refinement procedure as detailed above was used to obtain a converged 3D reconstruction.

3D Segmentation and Visualization. The final electron tomograms were segmented using *Amira* (Visage Imaging). 3D alignment and averaging were performed by using the fitting-map function in UCSF *Chimera* (7), the *proc3d* program in the EMAN package (6), and a custom-designed program called *alisum*. 3D visualization and surface rendering for both the averaged tomograms and single-particle reconstruction were performed using UCSF *Chimera* (7).

1. Kang X, et al. (2005) Reconstitution of uridine-deletion precleaved RNA editing with two recombinant proteins. *Proc Natl Acad Sci USA* 102:1017–1022.
2. Igo RP, Palazzo SS, Burgess ML, Panigrahi AK, Stuart K (2000) Uridylate addition and RNA ligation contribute to the specificity of kinetoplastid insertion RNA editing. *Mol Cell Biol* 20:8447–8457.
3. Kang X, et al. (2006) Reconstitution of full-round uridine-deletion RNA editing with three recombinant proteins. *Proc Natl Acad Sci USA* 103:13944–13949.
4. Bienvenut WV, et al. (2002) Matrix-assisted laser desorption/ionization-tandem mass spectrometry with high resolution and sensitivity for identification and characterization of proteins. *Proteomics* 2:868–876.
5. Winkler H, Taylor KA (2006) Accurate marker-free alignment with simultaneous geometry determination and reconstruction of tilt series in electron tomography. *Ultramicroscopy* 106:240–254.
6. Ludtke SJ, Baldwin PR, Chiu W (1999) EMAN: Semi-automated software for high resolution single particle reconstructions. *J Struct Biol* 128:82–97.
7. Pettersen EF, et al. (2004) UCSF Chimera—a visualization system for exploratory research and analysis. *J Comput Chem* 25:1605–1612.

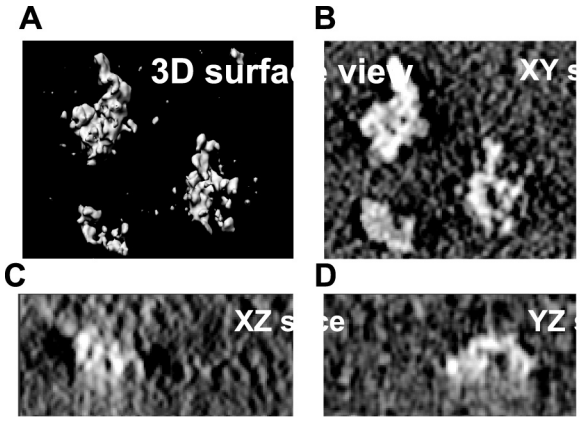

Fig. S1. Segmentation of the 3D tomogram showing well defined density boundaries in 3 dimensions. (*A*) 3D surface view. (*B*) XY slice through *A*. (*C*) XZ slice. (*D*) YZ slice. Sections from these tomograms revealed densities well above background, permitting the segmentation of individual L-complex particles for further 3D structural comparison at a resolution of ≈30–40 Å.

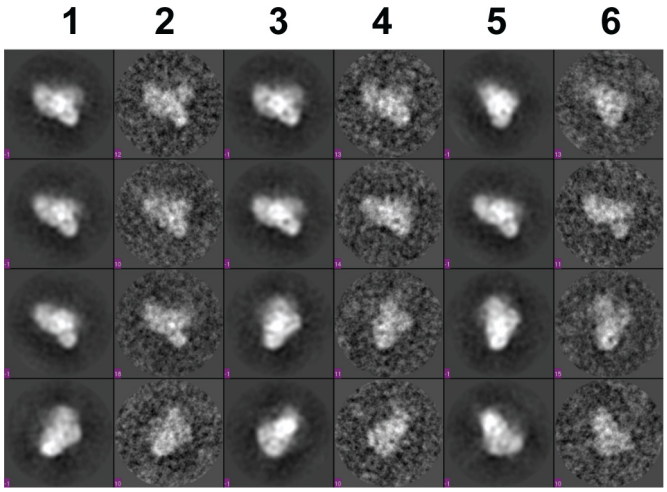

Fig. S2. Comparison of representative 2D projections and corresponding class averages. The 2D projections were obtained by projecting the unbiased single-particle reconstruction shown in Fig. 5*B* along the same orientation of the class averages. The close resemblance between the 2D projection and the class average supports the validity of the reconstruction. Lanes 1, 3, and 5, projections; lanes 2, 4, and 6, respective class averages.

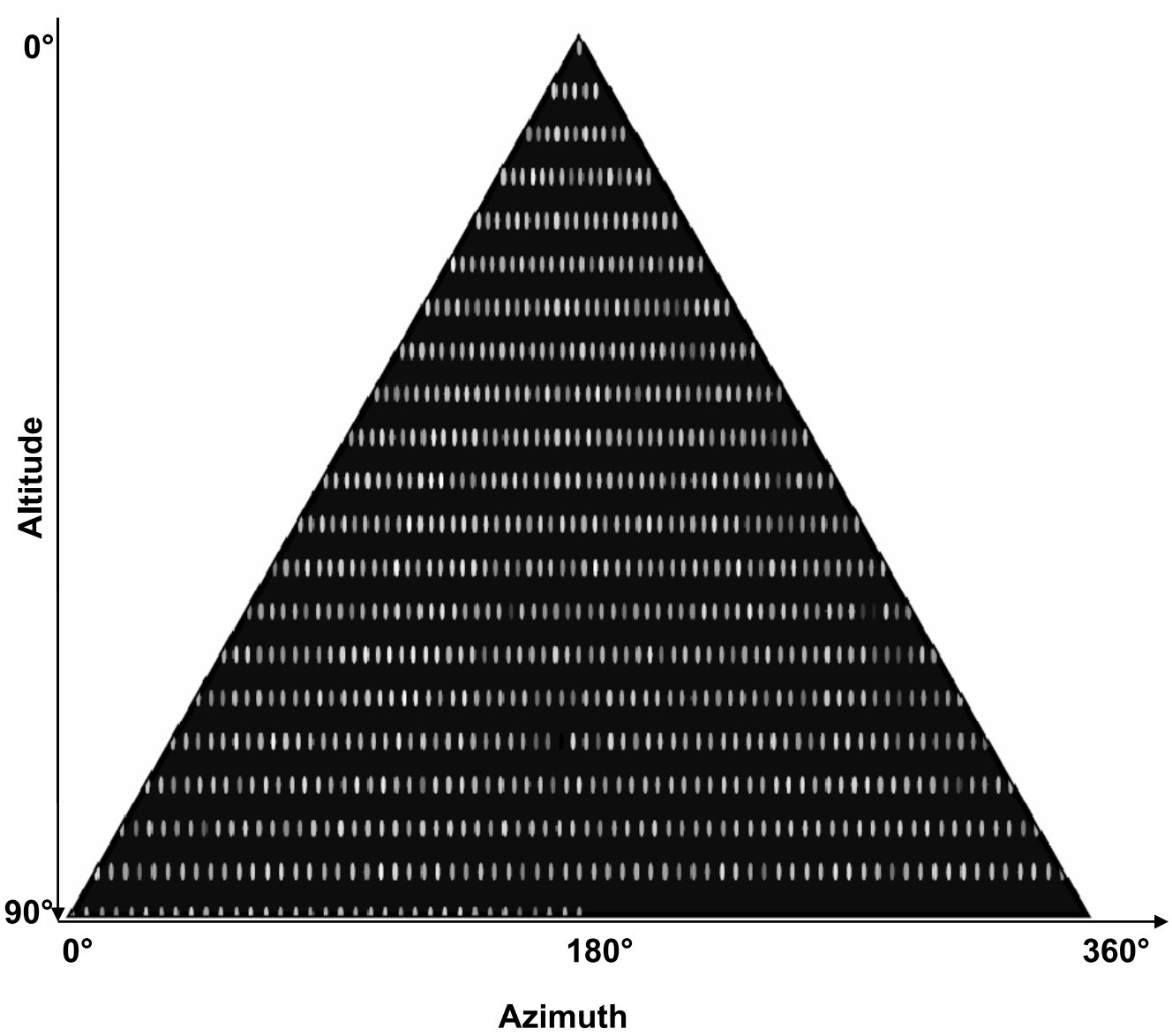

Fig. S3. Orientation distribution of single-particle reconstruction. Each oval represents a single class at a specific orientation. The brightness of the oval is in proportion to the number of particle images in that class.

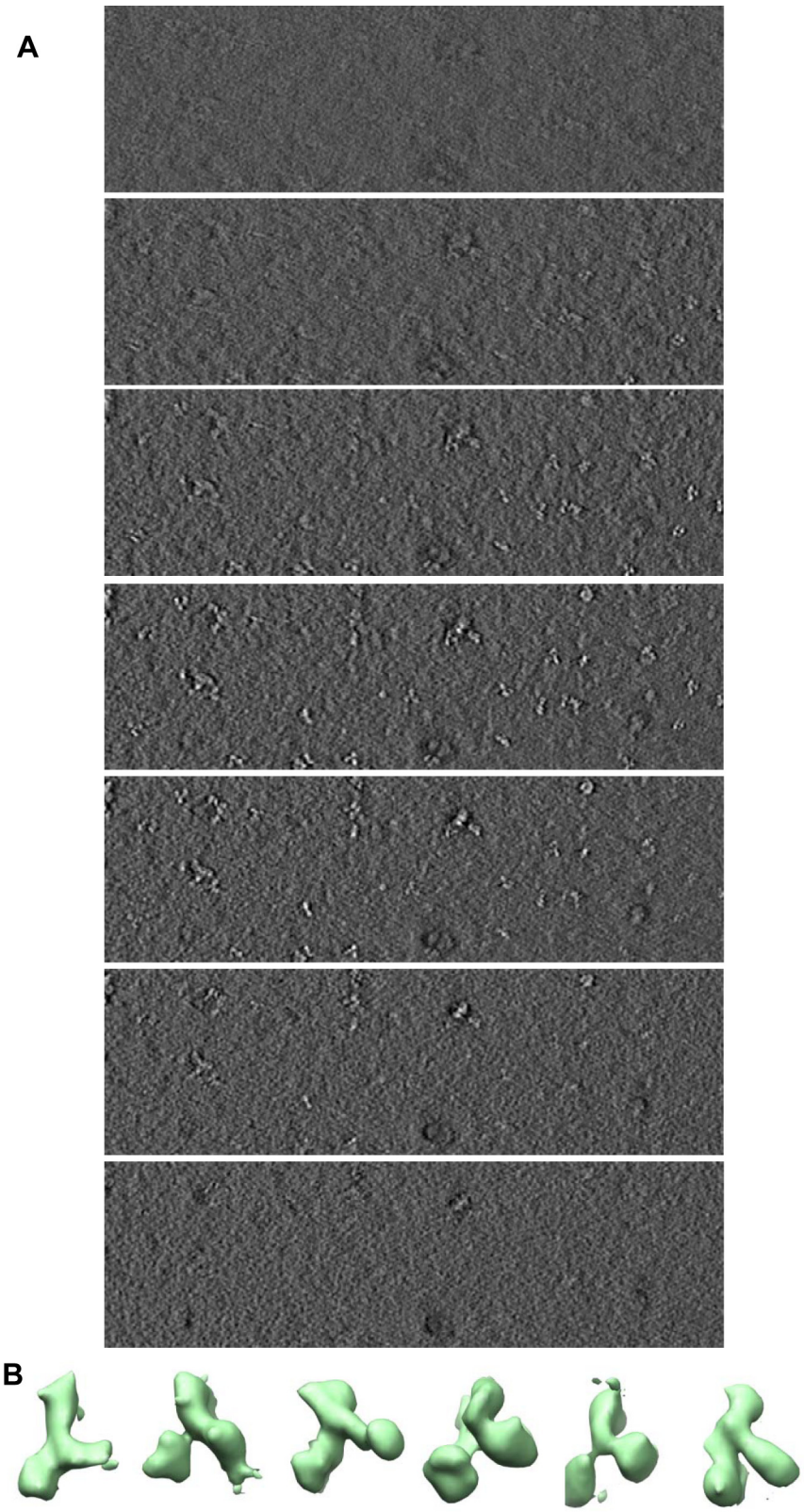

Fig. S4. Tomographic reconstruction of the 140-kDa IgG molecule. (*A*) Representative slices of IgG 3D tomogram. (*B*) Representative IgG particles segmented from 3D tomogram.

Table S1. L-complex polypeptides

Functional name	MP name	KRExx name	MW, −mito signal	Amino acids	Mitosignal
REL1	MP52	KREL1	49,768	449	
REL2	MP48	KREL2	45,378	400	
REX1	MP100	KREPC1	108,170	984	
REX2	MP99	KREPC2	72,375	676	
REN1*	MP90	KREPB1	94,425	870	No mitosignal
REN2†	MP61	KREPB3	58,085	512	
REN3‡	MP67	KREPB2	62,761	563	No mitosignal
RET2	MP57	KRET2	55,303	487	
LC1	MP81	KREPA1	97,831	943	
LC4	MP63	KREPA2	57,897	548	
LC5	MP46	KREPB4	54,296	496	
LC7B	MP42	KREPA3	47,431	431	
LC7C‡	MP49	KREPB6	48,425	439	
LC8-CBP	MP44	KREPB5	47,290	416	No mitosignal
LC10	MP24	KREPA4	25,847	240	
LC11	MP18	KREPA6	16,974	156	
MP41*	MP41	KREPB8	40,325	359	
MP47†	MP47	KREPB7	54,609	495	
SUM-REN1 complex			813,310		
SUM-REN2 complex			791,254		
SUM-REN3 complex			847,773		

The three nomenclatures are shown for the 18 *L. tarentolae* proteins generally accepted to be components of the complex. The molecular weights shown are without the putative mitochondrial signal sequences; three proteins have no predicted mitochondrial signal sequence. The LC-8 protein molecular weight includes the CBP tag. The molecular weights of the three classes of L-complexes (REN1, REN2, REN3) are indicated.

*REN1complex (REN1 + MP41).

†REN2 complex (REN2 + MP47).

‡REN3 complex (REN3 + LC7C).

Table S2. Proteins identified in LC8 TAP-purified complex

Protein name	Number of hits
REX1	3
REX2	11
REN2	7
RET2	5
REL1	3
REL2	6
LC-1	4
LC-4	4
LC-5	6
LC-7b	1
LC-8-CBP	4
LC-10	5
LC-11	6
MP19	3
REN3	1
LmjF20.0860	4
LmjF09.0190	3

Proteins in bold were previously identified in the REL1-TAP-purified complex. The number of peptides identified by mass spectrometry are shown in the right column. Proteins in normal font were not identified previously in the *L. tarentolae* REL1-TAP pull-down.